

# RSC Advances



This is an *Accepted Manuscript*, which has been through the Royal Society of Chemistry peer review process and has been accepted for publication.

*Accepted Manuscripts* are published online shortly after acceptance, before technical editing, formatting and proof reading. Using this free service, authors can make their results available to the community, in citable form, before we publish the edited article. This *Accepted Manuscript* will be replaced by the edited, formatted and paginated article as soon as this is available.

You can find more information about *Accepted Manuscripts* in the [Information for Authors](#).

Please note that technical editing may introduce minor changes to the text and/or graphics, which may alter content. The journal's standard [Terms & Conditions](#) and the [Ethical guidelines](#) still apply. In no event shall the Royal Society of Chemistry be held responsible for any errors or omissions in this *Accepted Manuscript* or any consequences arising from the use of any information it contains.

## Formation and oxygen diffusion barrier properties of fish gelatin/natural sodium montmorillonite clay self-assembled multilayers onto the biopolyester surface

Daniela Enescu,<sup>a\*</sup> Alberto Frache,<sup>b</sup> and Francesco Geobaldo<sup>b</sup>

### ABSTRACT

In order to expand the application of bio-derived polymers it is imperative that the issues related to their poor gas barrier properties be addressed. Here we explore the sequential layer by layer electrostatic self-assembly approach (abbrev. LbL) for modifying the oxygen transmission rate (OTR) of biopolyester with the trademark-FF 1482<sup>®</sup> (abbrev. BP) by deposition of fish gelatin/natural montmorillonite clay (trademark - Cloisite Na<sup>+</sup>, abbrev. CloNa<sup>+</sup>). We will show that the deposition of Fish gelatin/CloNa<sup>+</sup> onto the BP surface is influenced by different process parameters such as dipping time, drying step, polyelectrolyte concentration and surface activation of the BP film via partial alkaline hydrolysis as well as via low pressure plasma. Micro-attenuated total reflectance fourier-transform infrared spectroscopy (mATR-FTIR) and scanning electron microscopy/energy dispersive spectroscopy (SEM/EDS) showed that the traditional dipping LbL technique, which consist in keeping the film wet throughout all deposition cycle, led to a heterogeneous multilayers structure. The addition of the drying step has resulted to be a crucial parameter to obtain a quite homogenous Fish gelatin/CloNa<sup>+</sup> multi-layered structure. Further, the homogeneity of multi-layered structure was considerable improved when both CloNa<sup>+</sup> concentration was increased and the BP film surface was activated.

---

<sup>a</sup>The Centre for Research on Adaptive Nanostructure and Nanodevice, CRANN, Trinity College, Dublin 2, Ireland

<sup>b</sup>Department of Applied Science and Technology, Polytechnic of Turin, Corso Duca degli Abruzzi 24, Turin, Italy

By exploiting these processing parameters we were able to achieve successful homogenous Fish gelatin/CloNa<sup>+</sup> multi-layered structure as shown by SEM/EDS analysis. Further, the optimised samples showed a drastically decrease of OTR. For example, the OTR value for the sample, in which the BP surface was activated via plasma treatment prior to deposition of Fish gelatin/CloNa<sup>+</sup>, was reduced by 97% of the corresponding value of untreated BP film. This remarkable barrier may be attributed to a greater dispersion of the impermeable inorganic CloNa<sup>+</sup> platelets which forces the oxygen molecules to diffuse around them rather than taking a straight line pathway that lies perpendicular to the film surface. Thus, the results is a long and tortuous pathway for oxygen molecules diffusion through the multilayered structure formed.

**Keywords:** biopolyester, fish gelatin, montmorillonite, layer by layer assembly, oxygen diffusion barrier

## 1. INTRODUCTION

Bio-derived polymers due to their biodegradable nature have received considerable attention in the last two decades as a solution to minimize the environmental impact (i.e. it could at least to some extent solve the waste problem) of petroleum-derived polymers which are practically *undegradable*. These bio-derived polymers have found applications in the field of packaging<sup>1-12</sup> automotive<sup>13-15</sup> and biomedical.<sup>16-21</sup>

Referring to the biopolymer-based packaging, although they have advantages over their petroleum –based plastic competitors, nevertheless, their use is strongly limited because of the poor gas and water vapor barrier properties. To overcome these limitations, recently research studies<sup>22-25</sup> shown an interesting way to create high-performance materials for food and pharmaceutical packaging by applying layer by layer self-assembly concept. This concept, first proposed by Iler<sup>26</sup> in 1966, and then rediscovered by Decher and co-workers<sup>27-30</sup> 20 years ago, consists in the build-up of polyelectrolyte multilayer thin films onto solid substrate; the build-up is achieved through sequential and repetitive dipping of the substrate into aqueous solution of positively and negatively-charged polyelectrolytes. The main driving force for multilayer build-up is the electrostatic attraction, nevertheless, other interaction such as hydrophobic<sup>31,32</sup> and hydrogen bond donor and acceptor<sup>33-37</sup>, may also play a significant role under certain conditions. This LbL assembly technique is very simple in operating process and can be easily scaled up<sup>28,38,39</sup>. In addition, it is applicable for almost any type of charged species, such as nanoplates,<sup>40</sup> nanoparticles,<sup>41</sup> nanotubes,

<sup>42</sup> organic dyes,<sup>43</sup> dendrimers,<sup>44</sup> porphyrins,<sup>45</sup> biological polysaccharides,<sup>46,47</sup> nucleic acids and DNA,<sup>48</sup> viruses,<sup>49</sup> proteins,<sup>50-53</sup> and polypeptides.<sup>54, 55</sup>

In this context, the purpose of this investigation was to take the advantage of LbL concept in order to produce high oxygen barrier nano-multilayer films, based on fish gelatin/natural montmorillonite clay, onto the biopolyester film surface (biopolyester with the trademark-FF 1482<sup>®</sup>). To achieve this goal the optimization of LbL process parameters, such as dipping time, drying step, polyelectrolyte concentration and surface activation of the BP film via alkaline hydrolysis as well as via low pressure plasma, was carried out.

Fish gelatin is a mixture of water-soluble polypeptides derived from collagen by partially hydrolysis, with a range of both hydrophobic and hydrophilic side chains and over a wide range of pH it behaves as a polyampholyte (acting either as an acid or as a base). It was used as oppositely charged polyelectrolyte for CloNa<sup>+</sup>. In addition, it revealed lower oxygen permeability properties than those of mammalian gelatin films.<sup>56</sup>

Unmodified montmorillonite is a hydrated magnesium aluminum silicate layered clay, which belongs to the general family of 2:1 layered silicates. Its crystal structure consist of an edge-shared octahedral sheet of either magnesium or aluminum hydroxide between two silica tetrahedral layers.<sup>57,58</sup> The imbalance of the surface negative charges is compensated by exchangeable cations (Na<sup>+</sup>). The parallel layers are linked together by weak electrostatic forces.<sup>59</sup> Hence, its impermeable inorganic crystal structure is expected to cause a decrease in permeability of gases, in other words the gas molecules are forced to diffuse around this impermeable inorganic crystals rather than taking a straight line path that lies perpendicular to the film surface. Thus, the results is a long, tortuous pathway for gas diffusion through the film in the presence of it as illustrated in Fig. 1.

Fig. 1

## 2. EXPERIMENTAL SECTION

### 2.2. Materials

Biopolyester (trademark - FF 1482<sup>®</sup>, abbrev. BP) supplied by Novamont<sup>®</sup> (Italy) in film form and used as substrate for layer by layer deposition. Fish gelatin (Nr. G7765) from cold water fish skin, concentration ~45% in water was purchased from Sigma-Aldrich<sup>®</sup>. Unmodified montmorillonite clay (trademark - Cloisite Na<sup>+</sup>, abbrev. CloNa<sup>+</sup>) was purchased from Southern Clay Products<sup>®</sup> (Texas, USA), whose specific gravity is 2.86 g/cm<sup>3</sup>, diameter of 10-100 nm, thickness of 1 nm<sup>61,62</sup> and a cationic exchange capacity of 92 mequiv/100 g of CloNa<sup>+</sup>,<sup>63</sup> in deionized water is negatively-

charged. Sodium hydroxide (NaOH) was purchased from Sigma-Aldrich<sup>®</sup>. The water used for all preparation procedures was obtained from Milipore purification system (Milli Q).

### 2.1. LbL deposition

Different process parameters such as dipping time, drying step, polyelectrolyte (abbrev. PE) concentration and BP film surface activation via partial alkaline hydrolysis as well as via low pressure cold plasma were investigated and optimized in order to achieved a uniform deposition of PEs onto the BP film surface. Therefore, below are reported different LbL deposition procedures:

#### Procedure 1

##### Solutions Preparation and LbL assembly of Fish gelatin/CloNa<sup>+</sup> films

2 g CloNa<sup>+</sup> were dispersed into 1 L deionized water to prepare a 0.2 wt.% nanoclay suspension. The suspension was vigorously stirred in a flask equipped with a magnetic stir bar for 14 hours at room temperature; the pH of nanoclay suspension was 9.26 at 30 °C. Fish gelatin solution (0.3 wt.%) was stirred for 14 hours at room temperature; the pH of the solution was 5.17 at 29 °C, no pH adjustment of both solutions was performed.

BP film was dipped into fish gelatin aqueous solution and held for 5 minutes to deposit a layer of fish gelatin followed by rinsing with deionized water with aimed to remove the excess of fish gelatin. In addition, rinsing plays the key role in LbL assemblies because it results in precise nanoscale thickness control. The fish gelatin-covered substrate was subsequently dipped into nanoclay aqueous suspension and held for 5 minutes to deposit a layer of nanoclay on top of fish gelatin layer followed by rinsing with deionized water. The deposition process of fish gelatin/nanoclay layers in a cyclic fashion was repeated until the desired number of bilayers was reached, with the difference that the immersion time in solutions of the steps subsequent towards to the first one was only 1 minute. With this procedure were build-up 5, 10 and 20, respectively bilayers (each positive and negative pair deposited of a cycle is referred as a bilayer; abbrev. BL ) and reported as BP\_1\_5BL, BP\_1\_10BL and BP\_1\_5BL, respectively.

#### Procedure 2

Fish gelatin/CloNa<sup>+</sup> multilayers deposition was carried out applying *Procedure 1*, with the exception that the dipping time in the PEs aqueous solutions was increased to 15 minutes for each step. With this procedure 12 BL were build-up and reported as BP\_2\_12BL.

#### Procedure 3

This procedure differ of *Procedure 2* through that before each rinsing with deionized water, the specimen was dried with hot air (*hair dryer*) for 1 minute and 30 seconds. With this procedure 5BL and 8BL, respectively were build-up and reported as BP\_3\_5BL and BP\_3\_8BL, respectively.

#### **Procedure 4**

Fish gelatin/CloNa<sup>+</sup> multilayers deposition was carried out applying *Procedure 3*, with the exception that prior to the deposition process, an alkaline pre-treatment on the BP film surface was performed by immersing it into NaOH aqueous solution for 5 minutes at room temperature (0.4 wt.%; pH of the solution:12.81). In addition, the drying step was made in an oven at 40 °C for 5 minutes. With this procedure 5 BL were build-up and reported as BP\_4\_5BL.

#### **Procedure 5**

Concerning this procedure as compared with the others, the concentration of CloNa<sup>+</sup> was increased from 0.2 wt.% to 0.5 wt.%. The nanoclay suspension was vigorously stirred in a flask equipped with a magnetic stir bar for one week at room temperature; the pH of nanoclay suspension was 10.07 at 24°C, no pH adjustment of the nanoclay suspension was performed. Prior to start the deposition process, the nanoclay suspension was ultrasonicated for 30 minutes in order to improve the dispersion; in other words, we expect that the power of the ultrasonic waves to enhance breakup of layered silicate bundle.

BP film was dipped into fish gelatin aqueous solution and held for 10 minutes to deposit a layer of fish gelatin followed by drying with hot air for 1 minute and 30 seconds and then rinsing with deionized water. The fish gelatin-covered substrate was subsequently dipped into nanoclay aqueous suspension and held for 1 minute to deposit a layer of nanoclay on top of fish gelatin layer followed by drying with hot air for 1 minute and 30 seconds and rinsing with deionized water. These steps were repeated until the desired number of bilayers was reached. With this procedure 5 BL were build-up and reported as BP\_5\_5BL.

#### **Procedure 6**

This procedure differ of *Procedure 5* through that before the deposition process, the surface of BP film was activated via low pressure plasma treatment (Fig 2). With this procedure 5 bilayers were build-up and reported as BP\_6\_5BL\_Plasma 1 and BP\_6\_5BL\_Plasma 2, respectively. Plasma 1

and 2 respectively refers to the plasma exposure time (treatment time) which was 1 and 2 min, respectively.

Fig. 2

## 2.4. Characterization

### **Scanning electron microscopy (SEM)/energy-dispersive X-ray spectroscopy (EDS)**

The microstructural and elemental analyses of untreated BP film and multilayer films were carried out with a scanning electron microscope (LEO 1450 VP, Oberkochen, Germany) with an energy-dispersive X-ray probe (INCA Energy Oxford, UK) attachment. The surface as well as the cross-section of the samples were sputter-coated with gold for 27 s at a working pressure of 0.1 mbar before the SEM/EDS measurements to prevent the build-up of an electric negative charge in the specimen, which would induce “imaging artefacts” and to enhance resolution.

### **Micro-attenuated total reflection-fourier transform infrared (mATR-FTIR) spectroscopy**

mATR-FTIR spectra were recorded on a Frontier<sup>TM</sup> FT-IR spectrometer (Perkin Elmer, Germany). Each spectrum was recorded in a spectral range 4000-450  $\text{cm}^{-1}$ , 16 scans at 4  $\text{cm}^{-1}$  spectral resolution.

### **BP film surface pre-treatment via low pressure oxygen plasma**

Oxygen plasma treatment was performed in order to generate active site onto the BP film surface for the initial adsorption of polyelectrolyte chain. According to the literature,<sup>64-67</sup> the polar groups formed on the polymer surface via both energetic ion bombardment and surface oxidation by the reactive species present in the plasma contribute fundamentally in improving surface wettability, which in turn represent an important criterion for ensuring a good adhesivity in particular for immobilization of biological macromolecules (proteins, polysaccharide, etc.) onto different types of substrate surfaces.<sup>68,69</sup> Plasma treatment was conducted in a Diener Electronic GmbH, Series Pico (Germany) with a cylindrical chamber with capacity of 5 liters, semi-automatic control and plasma generator operating at 40 kHz with a maximum power of 200 W. The parameters were set as follow: oxygen plasma flow rate, pressure, and discharge plasma power were kept constant at: 20  $\text{cm}^3/\text{min}$ , 50 Pa, and 50 W respectively, whereas the plasma exposure time (treatment time) was 1 and 2 min, respectively.

### Water Contact angle measurements

Change in the BP film surface polarity due to the pre-treatment via partial alkaline hydrolysis as well as via low pressure plasma was measured according to the sessile-drop method using CAM 200 contact angle goniometer (KSV Instruments Ltd., Finland). The volume of the water drop used was 5  $\mu\text{L}$  in all measurements, therefore the effect of gravity is neglected (the gravity forces enhance the spreading of drop when the volume of it is between 30-50  $\mu\text{L}^{70}$ ). The water contact angle values are calculated by using the software of the instrument; all reported values herein are the average of three measurements taken at three different locations on each sample surface.

**Oxygen transmission rate (OTR)** was performed by MultiPerm-ExtraSolution<sup>®</sup> (Italy). OTR testing was done at 23 °C and 40% RH. The exposure area of the film was 50  $\text{cm}^2$ .

## 3. RESULTS AND DISCUSSION

Effect of different processing variables, such as dipping time, drying step, polyelectrolyte concentration and surface activation of the BP film via partial alkaline hydrolysis as well low pressure plasma, on the formation of Fish gelatin/ $\text{CloNa}^+$  multilayer films onto the BP film surface have been investigated. Further, the oxygen barrier properties were performed on the optimized samples.

### 3.1. Effect of dipping time

Taking into account that by changing the dipping time, it changes the time available for the polyelectrolyte molecules to arrange themselves on the substrate and *ionically* bond to the substrate surface, we examined first its effect on the formation of Fish gelatin/ $\text{CloNa}^+$  multilayer films onto the BP film surface by means of micro-attenuated total reflectance fourier-transform infrared spectroscopy and scanning electron microscopy/energy dispersive spectroscopy.

As Fig 3. shows, the characteristic infrared absorption bands of  $\text{CloNa}^+$  appear at 3626  $\text{cm}^{-1}$  due to O-H stretching vibration for Si-Si-OH, a broad band centered at 3387  $\text{cm}^{-1}$  due to interlayer and H-bonded -OH stretching vibration, at 1634  $\text{cm}^{-1}$  is attributed to the water of crystallization bending vibration, at 1118  $\text{cm}^{-1}$  due to Si-O bending vibration, at 1007  $\text{cm}^{-1}$  due to Si-O stretching vibration,

at  $915\text{ cm}^{-1}$  and  $796\text{ cm}^{-1}$  due to Al-Al-OH and Al-Mg-OH bending vibrations and at  $519\text{ cm}^{-1}$  due to the Si-O-Al bending vibrations. The infrared spectrum profile is in agreement with those reported in the literature.<sup>71-73</sup>

Fish gelatin revealed absorption bands at  $3275\text{ cm}^{-1}$  due to NH stretching vibration, at  $1631\text{ cm}^{-1}$  attributed to amide I, CO and CN stretching vibration, at  $1546\text{ cm}^{-1}$  ascribed to amide II and at  $1246\text{ cm}^{-1}$  due to amide III (Fig.3).<sup>74</sup>

Fig. 3

Taking into account the above information about the vibrational assignments of the infrared active bands of PEs and comparing with BP\_1\_5BL, 10BL, and 20BL obtained by applying *Procedure 1*, the spectra (*data not shown*) revealed that the deposition of PEs did not occurred. mATR-FTIR support SEM/EDS analyses (*data not shown*) in which the parameters used in *Procedure 1* did not favor the deposition of PEs. This situation changes, but not in significant manner, when the dipping time in aqueous polyelectrolytes solutions is increased to 15 minutes, with all others parameters kept constant (*see Experimental Section, Procedure 2*). The mATR-FTIR spectrum of BP\_2\_12BL, although is very similar in shape to that of untreated BP film (Fig. 4) showed an increasing in the intensity of the absorption bands in the  $1120\text{-}500\text{ cm}^{-1}$  region, which indicates the presence of CloNa<sup>+</sup> in BP\_2\_12BL. The amount of nanoclay present is extremely limited. In addition, the morphologies observed in Fig. 5b and 5c correlate well with mATR-FTIR analysis, in which the increase of dipping time has resulted in the formation of a heterogeneous layered structure.

Figure 4

Figure 5a,b,c

### 3.2. Effect of drying step

To increase the deposition of polyelectrolytes onto the BP surface, a partial drying step was applied (*see Experimental Section, Procedure 3*). The results on Fish gelatin/CloNa<sup>+</sup> multilayers deposition onto the BP film surface in the presence of drying step are shown in Fig. 6; mATR-FTIR spectra of BP\_3\_5BL and 8BL, respectively revealed the presence of CloNa<sup>+</sup> by the appearance of absorption bands at  $3626\text{ cm}^{-1}$  and in the  $1120\text{-}500\text{ cm}^{-1}$ . The presence of PE was confirmed also by the decrease in the absorption intensities of the bands characteristic of untreated film and, furthermore,

the decrease was higher for coating with 8 cycles of Fish gelatin/CloNa<sup>+</sup> multilayer films than for coating with 5 cycles, pointing out that the coating thickness is greater. Additionally, it was revealed a broad band between 3550 and 3150 cm<sup>-1</sup> assigned to the H-O-H stretching vibration of free H<sub>2</sub>O adsorbed onto the structure and/or inter-laminar water.

Fig. 6

The SEM/EDS data verified the successful deposition of Fish gelatin/CloNa<sup>+</sup> multilayer films. The SEM micrographs of BP\_3\_5BL (Fig. 7a) showed a uniform distribution of CloNa<sup>+</sup>, but in terms of dispersion revealed the presence of aggregates, the bright spots on the backscattered images, distributed all over the matrix, with some of them having diameters up to 5.8 μm. The micrographs of the cross-sectional morphology (Fig. 7b, c) revealed a uniform layered structure. The thickness of this layered structure perceivable at 20.00kx magnification was estimated to be about several hundred nanometers.

Fig. 7a, b, c

When the number of deposition cycles increased from five to eight, SEM micrographs (Fig. 8a) revealed the presence of CloNa<sup>+</sup> in large quantity onto the BP film surface and this is confirmed also by EDS mapping (the quantity of silicon and aluminum onto the BP film surface is greater with increasing of bilayers number). Furthermore, as Fig. 8a shows there are areas where the deposition takes place more than others and besides this, Fig. 8b (secondary electrons) evidence that in some areas of film there is a crushing layer and detachment of the material deposited. This detachment of the material, in specific areas, it was confirmed also by cross-sectional micrographs (Fig. 8c,d). Based on these results it can be supposed that, after approximately 8 cycle application, the polyelectrolyte layer reaches its final saturated state.

Fig. 8 a,b,c,d

According to the literature,<sup>75-79</sup> numerous variables can affect the adsorbed gelatin amount and the structure gelatin layer onto a solid surface, such as pH, ionic strength, concentration of the solution, gelatin molecular weight and distribution, surface chemistry and temperature. Consequently, gelatin adsorption is a very complex process, which is driven by different forces such as hydrogen bonding<sup>80</sup>, hydrophobic<sup>81</sup> and electrostatic forces.<sup>82</sup>

Here, we show that the deposition of Fish gelatin/CloNa<sup>+</sup> onto the BP film surface can be drastically improved by adding drying step. This results suggest that fish gelatin adsorption at the first step is also caused by the hydrophobic interactions. The hydrophobic interactions takes place when hydrophobic domains or moieties are present on both the substrate surface and biomolecules of interest.<sup>83</sup> Hence, taking into account that the surface of biopolyester film used in this work is extremely hydrophobic (the water contact angle value is 104°) and gelatin is a weak polyampholytes with a nonuniform distribution of amino acids, containing both positively charged polar amino acids (arginine, lysine) and negatively charged amino acids (glutamate, aspartate) in addition to hydrophobic neutral amino acids (comprising leucine, isoleucine, methionine and valine); the positive: negative: hydrophobic moieties are present in the approximate ratio:1:1:1,<sup>83-86</sup> one can speculate that the drying process can promote hydrophobic interactions due the following reason:

in water, hydrophobic moieties of gelatin are most frequently buried to the interior of it because they are incapable of forming hydrogen bonds with water (the water molecules cannot “wet” them), instead the water molecules form a highly ordered shell (or “cage”) around the hydrophobic moieties due to their inability to form hydrogen bonds in all the directions. Taking into account that, in general, the driving force for protein adsorption is the increase in entropy of the water molecules upon adsorption,<sup>87</sup> hence, in order to gain the entropy, hydrophobic moieties are forced to merge to minimize the extent of the water molecules shell (in other words hydrophobic moieties are forced to join leading in this way to a decrease in the number of ordered water molecules). Thus, hydrophobic interaction depends on the behavior of the water molecules rather than on direct attraction between the hydrophobic moieties.

Hot air drying can induce a loss of structural water from gelatin and thus a structural re-arrangement of the gelatin molecules. Consequently, heat drying can be responsible for a closer position of hydrophobic moieties to the surface from which a better interaction results. This behavior is in agreement with the finding reported by Serizawa and co-workers on fabricated ultrathin polymer films via the repetition of the adsorption/drying processes, who also confirmed that drying after the deposition step of collagen onto a quartz crystal microbalance can promote the adsorption driven by hydrophobic effect due to the following reasons: “the adsorption amount increased with an increase in adsorption temperature, indicating the presence of the hydrophobic effect of collagen adsorption; during a drying process, relatively hydrophobic amino acid residues in collagen should rearranged near the surface to minimize the interfacial free energy between a collagen film and air; collagen is constructed mainly by hydrophobic amino acids such glycine, proline, and hydroxiprollyne”.<sup>31</sup>

### 3.3. Effect of alkaline pre-treatment

With the aim to reduce the inhomogeneity of the Fish gelatin/CloNa<sup>+</sup> deposition, prior to apply LbL self-assembly procedure, the surface of BP film was activated via a partial alkaline hydrolysis treatment (see *Experimental Section, Procedure 4*). As it is known, the ester linkages are cleaved via chemical hydrolysis, which results in the generation of new terminal (hydroxyl and carboxyl) groups. In consequence, an increased number of functional groups onto the BP film surface could enhance binding with fish gelatin. Alkaline pre-treatment conditions were set up so that complete hydrolysis did not occurred within 5 min. After pre-treatment, water contact angle measurements was applied to characterize the hydrophilicity of the BP film surface. A surface can be considered as hydrophilic if the value of the contact angle is less than 90°, whereas the surface is hydrophobic if the value of the contact angle is greater than 90°. The water contact angle value of the BP film surface after alkaline pre-treatment decreased from 104° to 95°; the slight decrease can be attributed to the very short treatment time (5 minutes). Further, mATR-FTIR spectrum had shown that the alkaline pre-treatment induce an increase in the intensity of the absorption bands as compare with untreated BP film, which it could suggest the involvement of ester groups in the chemical attack. Based on water contact angle value as well as mATR-FTIR analysis, it can be confirmed that alkaline pre-treatment induced changes only in the thin surface layer of BP film without altering the bulk properties.

Fig. 9

### 3.4. Deposition of Gelatin/CloNa<sup>+</sup> multilayer films onto the pre-treated BP film surface

We focused our attention in two spectral ranges, i) 3630-3150 cm<sup>-1</sup> and ii) 1120-500 cm<sup>-1</sup>. Which both are substantially modified by the presence of Clo Na<sup>+</sup>.

Upon inspection of Fig.10, is clear that the characteristic absorption bands of CloNa<sup>+</sup> are present in BP\_4\_5BL as follow: at 3626 cm<sup>-1</sup> due to the stretching vibration of the hydroxyl groups for Si-Si-OH; abroad band between 3550 and 3150 cm<sup>-1</sup> assigned to the H-O-H stretching vibration of free H<sub>2</sub>O adsorbed onto the structure and/or inter-laminar water, but the intensity is lower as compare to previous procedures. This reflects that the water is readily removable through drying in oven at 40 °C. A strong increase in the intensity of absorption bands in the 1120-500 cm<sup>-1</sup> region, due to the presence of CloNa<sup>+</sup>, was also revealed.

Fig. 10

Further evidence for the formation of Fish gelatin/CloNa<sup>+</sup> multilayer films onto BP film surface was obtained by SEM analysis. It shows a quite uniform distribution of nanoclay, but in terms of dispersion revealed the presence of aggregates distributed all over the matrix, with some of them having diameters up to 10.3 μm (Fig. 11a). By analyzing the cross-sectional SEMs in greater detail revealed the presence of a continuous, homogeneous multilayer film with the thickness above several hundred nanometers (Fig. 11b and c).

Fig. 11a,b,c

### 3.5. Effect of polyelectrolyte concentration

In comparison with the previous procedures, the concentration of CloNa<sup>+</sup> was increased from 0.2 wt.% to 0.5 wt.% while the concentration of fish gelatin was kept constant. Further, taking into account that the dipping time is concentration dependent, the total adsorption time of CloNa<sup>+</sup> was reduced from 15 min to 1 min and for fish gelatin from 15 min to 10 min (*see Experimental Section, Procedure 5*); in addition, a reduction of the dipping time to the minimum possible value increase high speed fabrication.

As shown in Fig.12, Fish gelatin/CloNa<sup>+</sup> adsorption onto the BP film surface is clearly identified by the characteristic absorption band of CloNa<sup>+</sup> at 3626 cm<sup>-1</sup> attributed to  $\nu$ Si-Si-OH vibration. Moreover a general and strong increase in the intensity of all the absorption bands characteristic of CloNa<sup>+</sup> and a notable decrease in the absorption intensity of the bands characteristic of untreated BP film were observed. Also in this case the broad band between 3550 and 3150 cm<sup>-1</sup> assigned to the H-O-H stretching vibration of free H<sub>2</sub>O was clearly visible.

Fig. 12

Further proof of the Fish gelatin/CloNa<sup>+</sup> adsorption onto the BP film surface was obtained by SEM/EDS analysis. The surface morphology of BP\_5\_5BL as observed by SEM micrographs and EDS mapping (Fig. 13a) is very similar to previous cases (*Procedure 3 and 4*), but the presence of CloNa<sup>+</sup> onto the BP film surface is distributed more evenly than in previous ones. The result also confirms that the level of CloNa<sup>+</sup> microdispersion obtained with this procedure is reduced significantly as compared to previous ones. The size of aggregates became much smaller when both

long-term stirring and ultrasonication were introduced. The size of clay aggregates greatly decreased to below 2.6  $\mu\text{m}$  which is much smaller size compared to previous procedures with short stirring time and without ultrasonication. During sonication the power of ultrasonic wave broke down the nanoclay aggregates to smaller sizes. In addition, a well-defined layered structure was revealed from the cross-sectional micrographs (Fig. 13b and c).

Fig. 13a,b,c

### 3.6. Effect of low pressure plasma pre-treatment

In order to enhance fish gelatin binding onto the BP film surface, prior to apply LbL self-assembly procedure, the BP film surface was activated by low pressure plasma treatment. The plasma is an ionized gas consisting of electrons, atomic ions, molecular ions and neutral atoms and/or molecules which upon collision with the surfaces of polymers placed in the plasma environment break down the covalent chemical bonds, thus creating free radicals on the polymers surface. Further, these free radicals will then undergo additional reactions, depending on the gases present in the plasma or subsequent exposure to gases in the atmosphere.<sup>88</sup>

### 3.7. Effect of oxygen plasma pre-treatment on hydrophilicity

It is very clear from Fig.14a that water contact angle decreases after plasma treatment, which imparts hydrophilic character to film surface due to formation of hydrophilic groups and which in turn it may be explained as follow: the oxygen plasma creates radical species in the molecular chains on the surfaces, mainly through molecular chain scission or hydrogen abstraction by bombardment of plasma particles (electronics, ions, and radicals:  $\text{O}_2 + \text{e} \rightarrow \text{O}_2^- \rightarrow \text{O} + \text{O}^-$ ,  $\text{e} + \text{O} \rightarrow \text{O}^+ + 2\text{e}$ ;  $\text{e} + \text{O}_2 \rightarrow \text{O}_2^+ + 2\text{e}$ ;  $\text{e} + 2\text{O}_2 \rightarrow \text{O}_2^- + \text{O}_2$ ,  $\text{O}_2^- + \text{O} \rightarrow \text{O}_3 + \text{e}$ ). The radical species that are created onto the polymer surface can then react with the various molecular and active species present in the plasma environment, thus the following oxidation reaction scheme it can be suggested:  $\text{RH} + \text{O} \cdot \rightarrow \text{R} \cdot + \cdot\text{OH}$ ,  $\text{R} \cdot + \text{O}_2 \rightarrow \text{RO}_2 \cdot$ ,  $\text{RO}_2 \cdot + \text{R}'\text{H} \rightarrow \text{RO}_2\text{H} + \text{R}' \cdot$ , where:  $\text{RO}_2\text{H}$  indicate the formation of acids, but the formation of alcohols, ethers, peroxide, hydroperoxides (not shown in this reaction scheme) are also possible. Therefore, these polar groups make the plasma treated BP surface become more hydrophilic compared to the untreated BP surface. We found that an extending of plasma processing time beyond 2 minutes leads only to a slight decrease of water contact value, thus suggesting that the BP surface has reached a limiting level of oxidation. Further, mATR-FTIR spectra (Fig. 14b) has shown a notable increase in the intensity of the absorption bands after oxygen

plasma treatment. Hence, we can expect that plasma pre-treatment to enhance fish gelatin binding onto the BP film surface.

Fig. 14a,b

### 3.8. Deposition of Fish gelatin/CloNa<sup>+</sup> multilayer films onto the pre-treated BP film surface

BP\_6\_5BL\_Plasma1 and BP\_6\_5BL\_Plasma2 as compared with untreated BP film (Fig.15) revealed an absorption band at 3626 cm<sup>-1</sup> due to  $\nu(\text{Si-Si-OH})$  as well as a strong increase in intensity of the absorption bands in the 1120-500 cm<sup>-1</sup> region, together with the broad band between 3550 and 3150 cm<sup>-1</sup> assigned to H<sub>2</sub>O.

Fig. 15

SEM micrographs of the multilayer films' cross-sections showed a well-defined layered structures (Fig. 16a, b). On the basis of these SEM data, it can be concluded that, indeed, the CloNa<sup>+</sup> platelets were successfully incorporated into the LbL structure.

Fig. 16

### Oxygen barrier of BP film coating with Fish gelatin/CloNa<sup>+</sup> multilayers thin films

Oxygen barrier performance were examined only on BP\_4\_5BL, BP\_5\_5BL, BP\_6\_5BL\_Plasma 1 and BP\_6\_5BL\_Plasma 1 as these samples revealed an uniform deposition of PEs onto the BP film surface as shown earlier. As Fig. 17 shows, the oxygen transmission rate (OTR) of BP film is drastically reduced upon coating with Fish gelatin/CloNa<sup>+</sup>. This remarkable barrier can be due to the CloNa<sup>+</sup> platelets which create a highly tortuous diffusion pathway for the oxygen molecules, in other words the oxygen molecules are forced to diffuse around these impermeable inorganic crystals rather than taking a straight line path that lies perpendicular to the film surface (*see Fig. 1*). Looking in further detail at the data of Fig.17 while keeping the deposition conditions of each coating in mind, makes it possible to make further observations. Comparing BP\_4\_5BL and BP\_5\_5BL thus shows the influence of CloNa<sup>+</sup> concentration; increasing CloNa<sup>+</sup> content from 0.2

wt.% to 0.5 wt.% appear to lead to a better barrier performance (OTR decreased up to 85% while for BP\_4\_5BL reached just 70%). This improvement indicates that a higher concentration of CloNa<sup>+</sup> platelets is necessary to increase the tortuosity of the diffusion pathway for the oxygen molecules.<sup>89</sup> Further, comparing the barrier performance of BP\_5\_5BL with BP\_6\_5BL\_Plasma1 (OTR: 92%) and P\_6\_5BL\_Plasma2 (OTR: 97%), it can be seen that a remarkable barrier improvement is only obtained when the BP film surface is activated by plasma treatment. In addition, it can be observed that increasing plasma treatment time leads to further enhancement of OTR value. Therefore, it can be assumed that oxygen plasma treatment has greatly enhanced the adhesion between polyelectrolyte and the BP film surface.

Fig. 17

#### 4. CONCLUSIONS

The results of this study show that, the Fish gelatin/CloNa<sup>+</sup> nanocoating onto the BP film surface using layer by layer deposition technique is sensitive to a number of processing conditions such as dipping time, drying step, polyelectrolyte concentration and surface activation of the BP film via alkaline hydrolysis as well as low pressure plasma. The deposition of Fish gelatin/CloNa<sup>+</sup> onto the BP film surface varied significantly when the above processing conditions were changed. The drying step, as revealed by SEM/EDS and mATR-FTIR analyses, has a great influence on the multilayer film formation, in other words it led to a quite uniform deposition of the PEs towards the procedure without drying step where a heterogeneous layered structure was formed. It was further found that the increase of polyelectrolyte concentration as well as surface activation of the BP film prior to be subjected to LbL process have a strong influence on the deposited 'film uniformity. By plasma surface activation a more uniform multilayered structure was formed, with a thickness of several hundreds of nanometers.

The samples which revealed an uniform deposition of Fish gelatin/CloNa<sup>+</sup> onto the BP film surface were further used to investigate the oxygen barrier properties. A remarkable decrease of oxygen transmission rate is achieved for all the sample (OTR decrease as follow: BP\_5\_5BL\_Plasma 2 < BP\_5\_5BL\_Plasma 1 < BP\_5\_5BL < BP\_4\_5BL; the level of decrease in OTR is 97%, 92%, 85% and 70%, respectively). This high barrier behavior may be attributed to the impermeable inorganic CloNa<sup>+</sup> platelets which forces the oxygen molecules to diffuse around them rather than taking a straight line pathway that lies perpendicular to the film surface (*see Fig.1*). Thus, the results is a long, tortuous pathway for oxygen molecules diffusion through the multilayerd structure formed.

As mentioned above, BP\_4\_5BL displayed the highest OTR value (679 cc/(m<sup>2</sup>· 24h)) towards other samples, which might be attributed to the low loading of nanoclay (0.2 wt.%), but by

increasing the nanoclay concentration (0.5 wt.%) a further decrease of OTR value is revealed ( $339\text{cc}/(\text{m}^2 \cdot 24\text{h})$ ). This improvement of the oxygen barrier indicates that a higher concentration of CloNa<sup>+</sup> platelets is necessary to increase the tortuosity of the diffusion pathway for the oxygen molecules.

Finally, the working conditions employed to prepare BP\_5\_5BL\_Plasma 1 and BP\_5\_5BL\_Plasma 2 were sufficient to allow efficient dispersion of CloNa<sup>+</sup> platelets providing thus a high resistance to the oxygen molecules diffusion ( $184$  and  $71\text{ cc}/(\text{m}^2 \cdot 24\text{h})$ , respectively).

In the light of the aforementioned findings and, also, taking into account the advantages of this method (easy to carry out, fast, versatile and ecofriendly), we concluded that Fish gelatin/CloNa<sup>+</sup> could be taken into consideration as nanocoating for BP film in order to improve the oxygen barrier.

### Acknowledgements

The authors thanks Italian Ministry of Economic Development (MISE) for the financial support for the Biopack project in the Industria 2015, "Bando Nuove Tecnologie per il Made in Italy" call.

### References

- 1 M.D. Sanchez-Garcia, A. Lopez-Rubio, J. M. Lagaron, *Trends Food Sci. Tech.*, 2010, **21**, 528-36.
- 2 K. Petersen, P.V. Nielsen, G. Bertelsen, M. Lawther, M. Olsen, N.H. Nilssonk, *Trends Food Sci. Tech.*, 1999, **10**, 52–68.
- 3 M.A. Cerqueira, A.C. Pinheiro, B.W.S. Souza, Á.M.P. Lima, C. Ribeiro, C. Miranda, *Carbohydr. Polym.*, 2009, **75**, 408–14.
- 4 A. Sorrentino, G. Gorrasi, V. Vittoria, *Trends Food Sci. Tech.*, 2007, **18**, 84-95.
- 5 S. Guilbert, N. Gontard, L.G.M. Gorris, *Food Sci. Tech.*, 1996, **29**, 10-17.
- 6 S. Guilbert, B. Cuq, N. Gontard, *Food Add. Contam.*, 1997, **14**, 741-51.
- 7 J. M. Lagaron, L. Cabedo, D. Cava, J. L. Feijoo, R. Gavara, E. Gimenez, *Food Add. Contam.*, 2005, **22**, 994-99.
- 8 M. Avella, J. J. De Vlieger, M. E. Errico, S. Fischer, P. Vacca, M. Volpe, *Food Chem.*, 2005, **93**, 467-74.
- 9 R. Aura, S. P. Singh, *J Test Eval.*, 2006, **34**, 530-36.
- 10 D. S. Rosa, N. T. Lotto, D. R. Lopes, C. G. Guedes, *Polym. Test*, 2004, **23**, 3-8.
- 11 S. Sinha Ray, M. Bousmina, *Prog. Mater. Sci.*, 2005, **50**, 962-1079.
- 12 S. Farrisa, K. M. Schaichb, L. Liuc, L. Piergiovannia, K. L. Yam, *Trends Food Sci. Tech.*, 2009, **20**, 316-32.

- 13 P. Lammers, K. Kromer, Competitive Natural Fiber Used in Composite Materials for Automotive Parts. ASAE Paper No. 026167. Chicago, Illinois. ASAE, 2002.
- 14 M. S. Hunda, L.T. Drzal, A. K. Mohanty, Misra M. 5<sup>th</sup> Annual SPE Automotive Composites Conference, sept, 12-14, 2005.
- 15 K. Troy, E. Michigan, M. Subyakto, E. Hermiati, N. Masruchin, K.W. Prasetyo, *Wood Res. J.* 2011, **2**, 21-26.
- 16 T. Kokubo, H. Kim, M. Kawashita, *Biomaterials*, 2003, **24**, 2161-175.
- 17 S. Sakiyama-Elbert, J. Hubbell, *Annu. Rev. Mater. Res.*, 2001, **31**, 183-201.
- 18 A. Jaklenec, E. Wan, M. E. Murray, E. Mathiowitz, *Biomaterials*, 2008, **29**, 185-92.
- 19 M. Skotak, A. P. Leonav, G. Larsen, S. Noriega, A. Subramanian, *Biomacromolecules*, 2008, **9**, 1902-908.
- 20 K. Ofiori-Kwakye, J. T. Fell, *Int. J. Pharm.*, 2003, **250**, 251-57.
- 21 P. Y. Li, P. S. Lai, W. C. Hung, W.J. Syu, *Biomacromolecules*, 2010, **11**, 2576–582.
- 22 A. J. Svagan, A. Åkesson, M. Cárdenas, S. Bulut, J. C. Knudsen, J. Risbo, D. Plackett, *Biomacromolecules*, 2012, **13**, 397–405.
- 23 T. Hirvikorpia, M. VähäNissia, A. Harlina, M. Salomäkib, S. Arevac, J. T. Korhonend, M. Karppinene, *Appl. Surf. Sci.*, 2011, **257**, 9451– 454.
- 24 G. Laufer, C. Kirkland, A. A. Cain, J. Grunlan, C. *Carbohyd. Polym.*, 2013, **95**, 299-302.
- 25 G. Laufer, M. A. Priolo, C. Kirkland, J. C. Grunlan, *Green Materials* 2012, **1**, 4-10.
- 26 R. K. Iler, *J Colloid Interface Sci.*, 1966, **21**, 569-94.
- 27 G. Decher, J. D. Hong, J. Schmitt, *Thin Solid Films*, 1992, **210/211**, 831-35.
- 28 G. Decher, *Science*, 1997, **277**, 1232-237.
- 29 G. Decher, M. Eckle, J. Schmitt, B. Struth, *Curr Opin Colloid Interface Sci.*, 1998, **3**, 32-39.
- 30 G. Decher, In multilayer thin films: sequential assembly of nanocomposites materials, Decher G. Schlenoff J.B., Wiley: Weinheim, 2003, pp. 1-46.
- 31 T. Serizawa, M. Akashi, *J. Polym. Sci. Part A Polym. Chem.*, 1999, **37**, 1903-906.
- 32 T. G. Shutava, S. S. Balkundi, Y. M. Lvova, *J. Colloid Interface Sci.*, 2009, **330**, 276–83.
- 33 W. B. Stockton, M. F. Rubner, *Macromolecules*, 1997, **30**, 2717-725,
- 34 I. Erel-Unal, S. A. Sukhishvili, *Macromolecules*, 2008, **41**, 8737–744.
- 35 V. Kozlovskaya, S. A. Sukhishvili, *Macromolecules*, 2006, **39**, 5569–572.
- 36 F. Boulmedais, M. Bozonnet, P. Schwinte, J. C. Voegel, P. Schaaf, *Langmuir*, 2003, **19**, 9873–882.
- 37 W. B. Stockton, M. F. Rubner, *Macromolecules*, 1997, **30**, 2717–725.
- 38 P. T. Hammond, *Curr Opin Colloid Interface Sci.* 1999, **4**, 430- 42.

- 39 P. T. Hammond, *Adv. Mater.*, 2004, **16**, 1271.
- 40 S. W. Keller, H. N. Kim, T. E Mallouk, *J. Am. Chem. Soc.*, 1994, **116**, 8817-818.
- 41 N. A. Kotov, I. Dekany, J. H. Fendler, *J Phys. Chem.*, 1995, **99**, 13065-3069.
- 42 A. A. Mamedov, N. A. Kotov, M. Prato, D. M. Guldi, J. P. Wicksted, A. Hirsch, *Nat. Mater.*, 2002, **1**, 190-94.
- 43 T. M. Cooper, A. L. Campbell, R. L. Crane, *Langmuir*, 1995, **11**, 2713-717.
- 44 J. A. He, R. Valluzzi, K. Yang, T. Dolukhanyan, C. Sung, J. Kumar, *Chem. Mater.*, 1999, **11**, 3268.
- 45 K. Araki, M. J. Wagner, M. S. Wrighton, *Langmuir*, 1996, **12**, 5393.
- 46 Y. Lvov, M. Onda, K. Ariga, T. Kunitake, *J. Biomater. Sci. Polym. Ed.*, 1998, **9**, 345.
- 47 L. Richert, P. Lavalle, D. Vautier, B. Senger, J. F. Stoltz, P. Schaaf, *Biomacromolecules*, 2002, **3**, 1170.
- 48 Y. Lvov, G. Decher, G. Sukhorukov, *Macromolecules*, 1993, **26**, 5396.
- 49 P. J. Yoo, K. T. Nam, J. Qi, S. K. Lee, J. Park, A. M. Belcher, P. T. Hammond, *Nat. Mater.* 2006, **5**, 234.
- 50 D. Hong, K. Lowack, J. Schmitt, G. Decher, *Prog Colloid Polym. Sci.*, 1993, **93**, 98.
- 51 Y. Lvov, K. Ariga, T. Kunitake, *Chem Lett.*, 1994, **12**, 2323-326.
- 52 Y. Lvov, K. Ariga, I. Ichinose, T. Kunitake, *J. Am. Chem. Soc.*, 1995, **117**, 6117-123.
- 53 W. Kong, X. Zhang, M. L. Gao, H. Zhou, W. Li, J. C. Shen, *Macromol. Rapid Commun.*, 1994, **15**, 405.
- 54 M. Mueller, *Biomacromolecules*, 2001, **2**, 262.
- 55 F. Boulmedais, V. Ball, P. Schwinte, B. Frisch, P. Schaaf, J. C. Voegel, *Langmuir*, 2003, **19**, 440.
- 56 J. B. Avena-Bustillos, B. Chiou, C. W. Olsen, P. J. Bechtel, D. A. Olson, T. H. McHuch, *J. Food Sci.*, 2011, **76**, E519-E524.
- 57 J. Weiss, P. Takhistov, D. J. McClements, *J Food Sci.*, 2006, **71**, R107-R116.
- 58 N. Salahuddin, A. Moet, A. Hiltner, E Baer, *European. J.*, 2002, **38**, 1477-482.
- 59 W. Tan, Y. Zhang, Y. S. Szeto, L. Liao, *Composites Sci. Techn.*, 2008, **68**, 2917-921.
- 60 T. V. Ducan, *J. Colloid Interface Sci.* 2011;doi:10.1016/j.jcis.2011.07.017
- 61 A. Sorrentino, G. Gorrasi, V. Vittoria, *Trends Food Sci. Techn.*, 2007, **18**, 84-95.
- 62 W. S. Jang, I. Rawson, J. C. Grunlan, *Thin Solid Films*, 2008, **516**, 4819-825.
- 63 M. Rodlerta, C. J. G. Plummera, L. Garamszegia, Y. Leterriera, H. J. M. Grunbauerb, Mansona J. E., *Polymer*, 2004, **45**, 949-60.

- 64 E. Occhiello, M. Morra, G. Morini, F. Garbassi, P. Humphrey, *J. Appl. Polym. Sci.*, 1991, **42**, 551.
- 65 S.Suzer, A. Argun, O. Vatanserver, O. Aral, *J. Appl. Polym. Sci.*, 1999, **74**, 1846.
- 66 S. Han, S. K. Koh, K. H. Yoon, *J. Electrochem Soc.*, 1999, **146**, 4327.
- 67 M. Kawabe, S. Tasaka, N. Inagaki, *J. Appl. Polym. Sci.*, 2000, **78**, 1392–401.
- 68 N. Dumitrascu, I. Topala, G. Popa, *IEEE Transactions on Plasma Sci.*, 2005, **33**, 1710-714.
- 69 L-C. Xu, C. A. Siedlecki, *Biomaterials*, 2007, **28**, 3273-283.
- 70 S. M. Kumar, A. P. Deshpande, *Colloids and Surfaces A: Physicochem Eng Aspects*, 2006, **277**, 157–63.
- 71 S. Mallakpour, M. Madani, *J. Mater. Sci.*, 2011, **46**, 4071-078.
- 72 J. Madejova, *Vibrational Spectroscopy*, 2003, **31**,1-10.
- 73 O. M. Sadek, W. K. Mekhemer, *Thermochimica Acta*, 2001, **370**, 57-63.
- 74 J. H. Muyonga, C. G. B. Cole, K.G. Duodu, *Food Chem.*, 2004, **86**, 325-332.
- 75 N. Likos, K. A. Vaynberg, H. Lo`wen, N. J. Wagner, *Langmuir*, 2000, **16**, 4100-108,
- 76 Y. Lin, L.Wang, P. Zang, X. Wang, X. Chen, X. Jing, Z. Su, *Acta Biomater.*, 2006, **2**,155-64.
- 77 W. F. Harrington, N. V. Rao, *Biochemistry*, 1970, **9**, 3714–724.
- 78 A. R. Mackie, A. P. Gunning, M. J. Ridout, V. J. Morris, *Biopolymers*, 1998, **46**, 245–52.
- 79 C. Joly-Duhamel, D. Hellio, M. Djabourov, *Langmuir*, 2002, **18**,7208–217.
- 80 M. Westwood, A.P. Gunning, R. Parker, *Macromolecules*, 2010, **43**, 10582–0593.
- 81 T. G. Shutava, S. S. Balkundi, Y. M. Lvova, *J. Colloid Interface Sci.*, 2009, **330**,276–83.
- 82 Y. Kamiyama, J. Israelachvili, *Macromolecules*, 1992, **25**, 5081-088.
- 83 D. Aronov, R. Rosen, E. Z. Ron, G. Rosenman, *Process Biochemistry*, 2006, **41**, 2367–372.
- 84 S. Chatterjee, H. B. Bohidar, *J. Surface Sci. Technol.*, 2006, **22**, 1-13.
- 85 K. A. Vaynberg, N. J. Wagner, R. Sharma, *Biomacromolecules*, 2000, **1**, 466-72.
- 86 Y. Kamiyama, J. Israelachvili, *Macromolecules*, 1992, **25**, 5081-088.
- 87 A. M. Abdul-Fattah, D. S. Kalonia, M. J Pikal., *J. Pharm Sci.*, 2007, **96**, 1886-916.
- 88 G. P. Hansen, R. A. Rushing, R. W. Warren, S. L. Kaplan, O. S. Kolluri, *Int .J. Adhes. Adhes .*, 1991, **11**, 247–54.
- 89 C. J. Grunlan, A. Grigorian, C. B. Hamilton, A. R. Mehrabi, *J. Appl. Polym. Sci.*, 2004, **93**, 1102–109.

- Fig. 1** Schematic illustration, adapted from Ducan,<sup>60</sup> of gas molecules diffusion through (a) a film composed only of polymer (gas molecules migrate via a pathway that is perpendicular to the film orientation) and (b) a nanocomposite film (gas molecules are forced to go around the impenetrable platelets and through interfacial zones which have different permeability characteristics than those of the neat polymer).
- Fig. 2** Schematic presentation of preparation of LbL - Fish gelatin/CloNa<sup>+</sup> nanocoating of PB film involving activation of the BP film surface via low pressure plasma followed by immersion of it into the polyelectrolytes aqueous solutions.
- Fig. 3** mATR-FTIR spectra of Fish gelatin and CloNa<sup>+</sup>.
- Fig. 4** mATR-FTIR spectra of the untreated BP film and BP\_2\_12BL.
- Fig. 5** Cross-sectional SEM micrographs of (a) untreated BP film and (b, c) BP\_2\_12BL.
- Fig. 6** mATR-FTIR spectra of CloNa<sup>+</sup>, untreated BP film, BP\_3\_5BL and BP\_3\_8BL.
- Fig. 7** (a) Surface and (b,c) cross-sectional SEM micrographs of BP\_3\_5BL.
- Fig. 8** (a, b) Surface and (c,d) cross-sectional SEM micrographs of P\_3\_8BL.
- Fig. 9** mATR-FTIR of the untreated BP film and the BP film pre-treated via alkaline treatment.
- Fig. 10** mATR-FTIR of the untreated BP film, CloNa<sup>+</sup> and BP\_4\_5BL.
- Fig. 11** (a) Surface and (b,c) cross-sectional SEM micrographs of BP\_4\_5BL.
- Fig. 12** mATR-FTIR of the untreated BP film, CloNa<sup>+</sup> and BP\_5\_5BL.
- Fig. 13** (a) Surface and (b,c) cross-sectional SEM micrographs of BP\_4\_5BL.
- Fig. 14** (a) Sessile-drop water contact angle onto the untreated BP film surface and plasma pre-treated BP film surface. (b) mATR-FTIR spectra of the untreated BP film and the plasma pre-treated BP film.
- Fig. 15** mATR-FTIR of the untreated BP film, CloNa<sup>+</sup> and BP\_6\_5BL\_Plasma1 and BP\_6\_5BL\_Plasma2.
- Fig. 16** Cross-sectional SEM micrographs of (a) BP\_6\_5BL\_Plasma1 and (b) BP\_6\_5BL\_Plasma2.
- Fig. 17** Oxygen transmission rate for the untreated and nanocoated BP film.

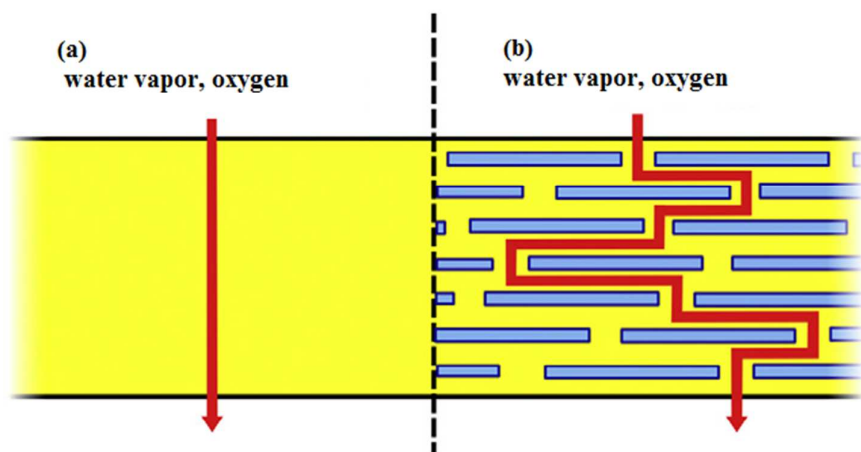


Figure 1

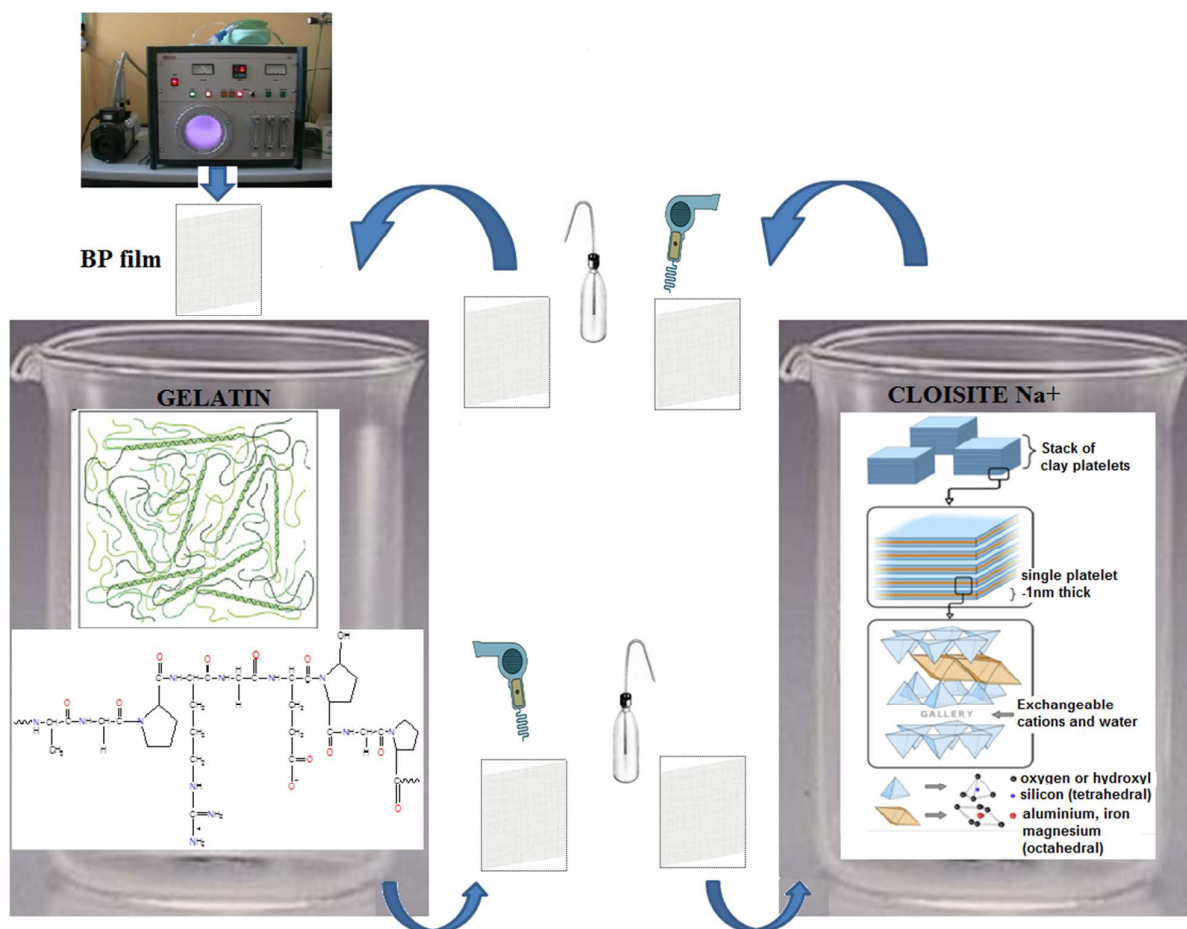


Figure 2

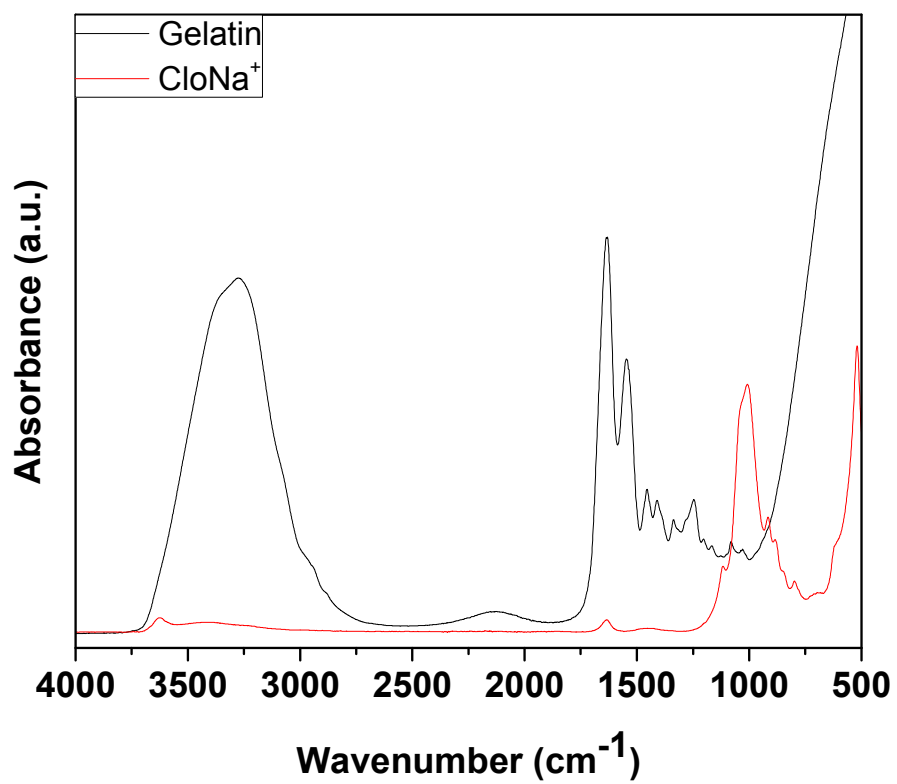


Figure 3

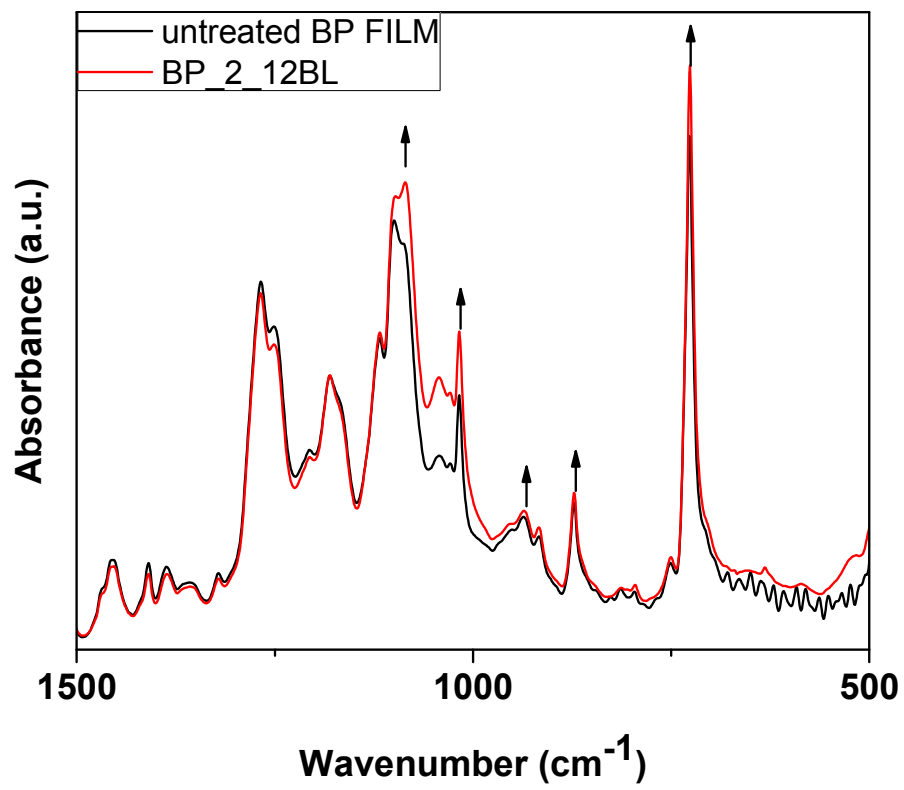


Figure 4

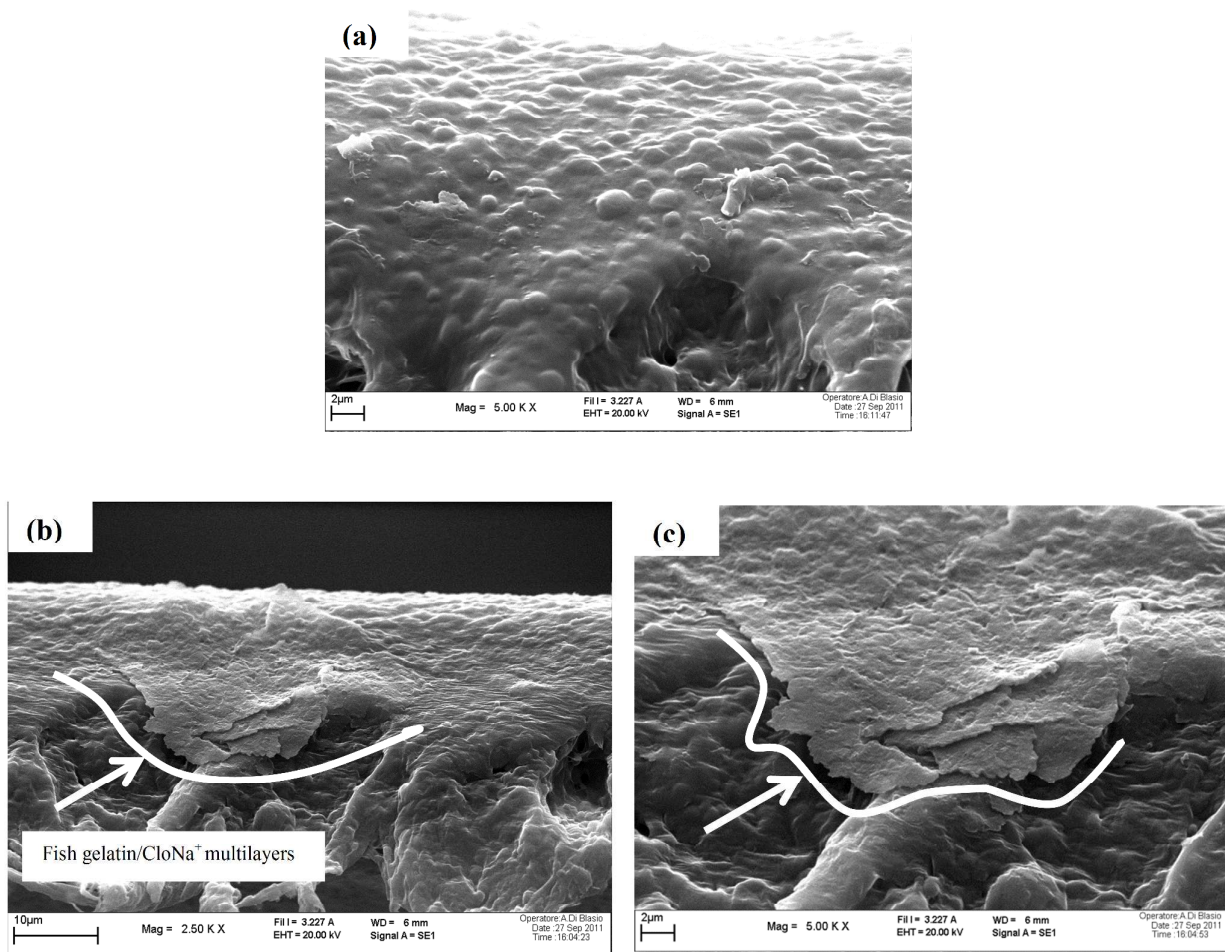
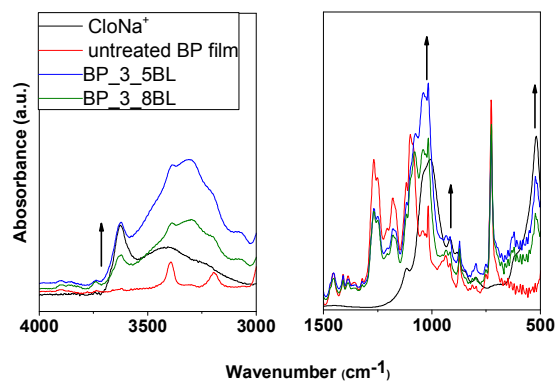


Figure 5

**Figure 6**

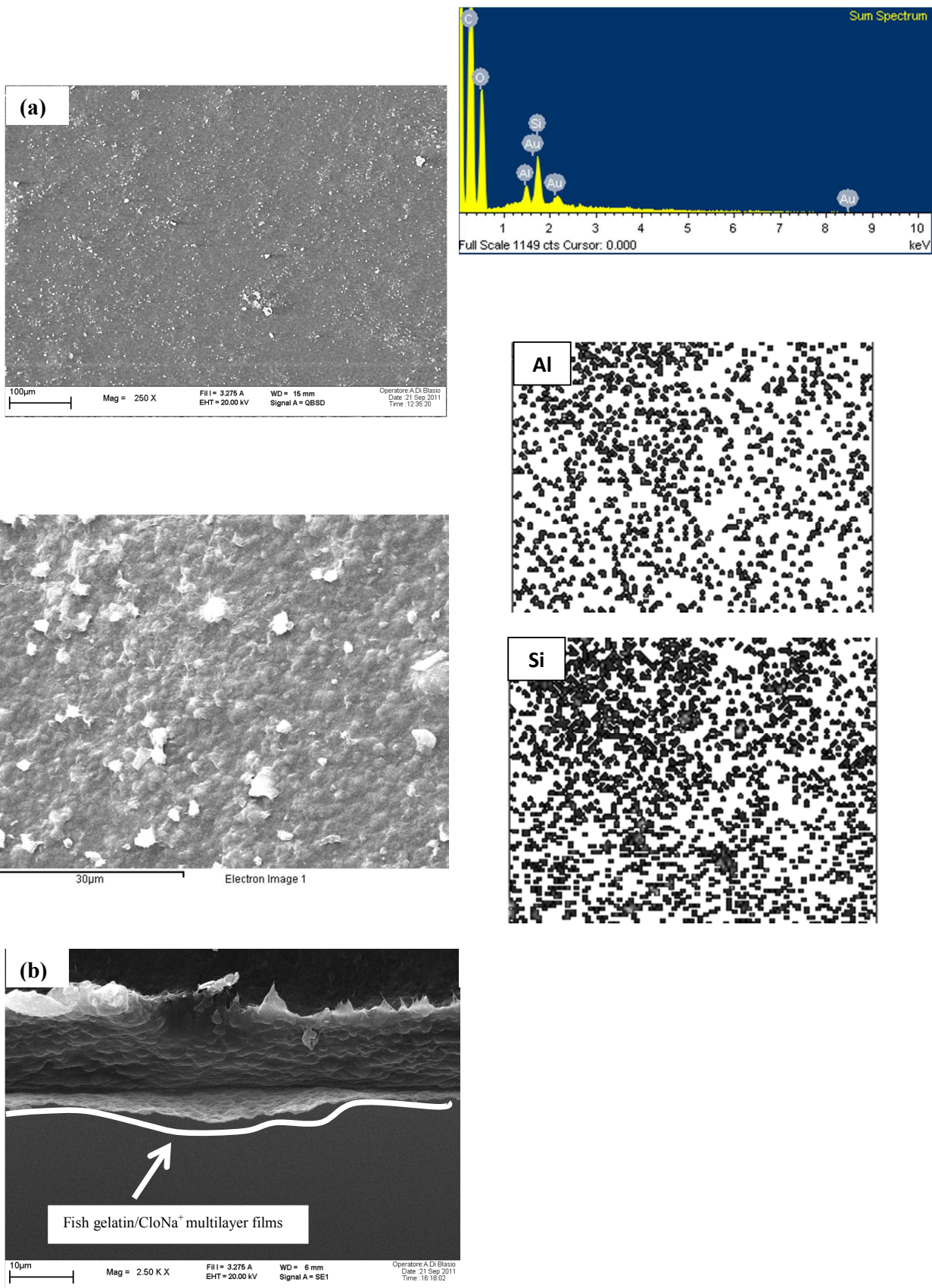
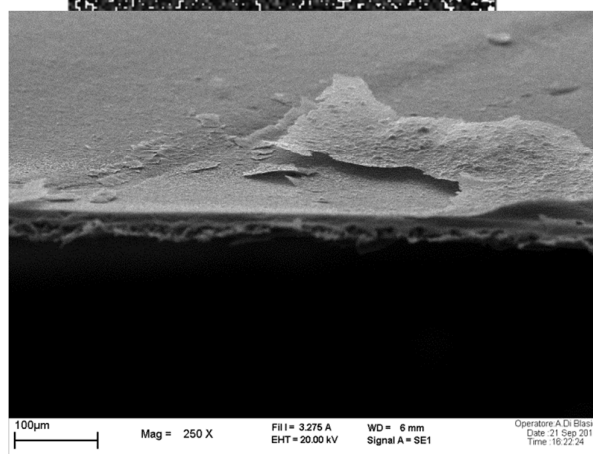
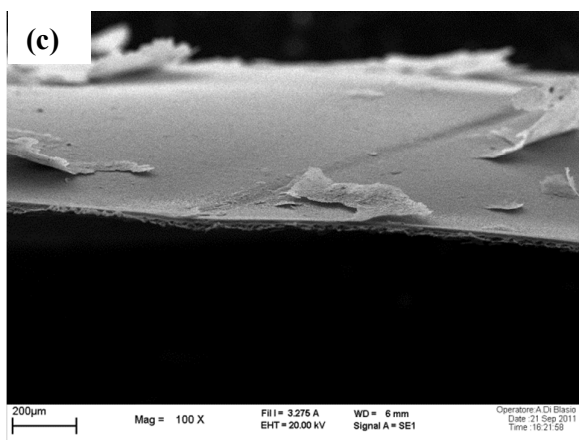
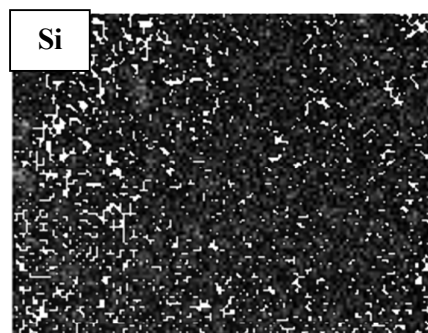
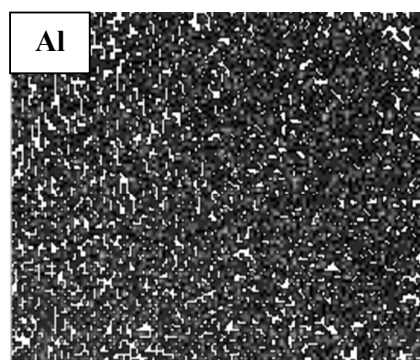
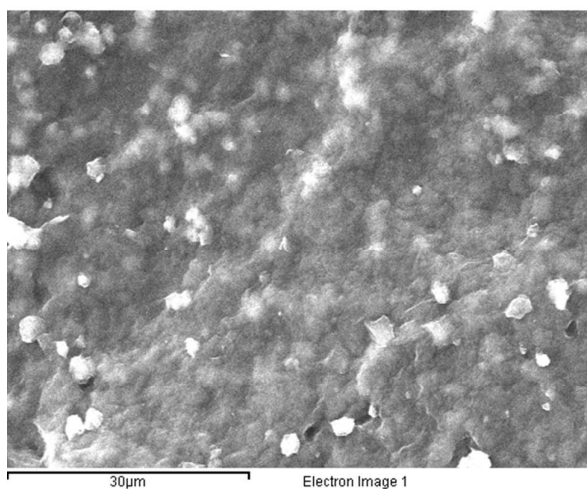
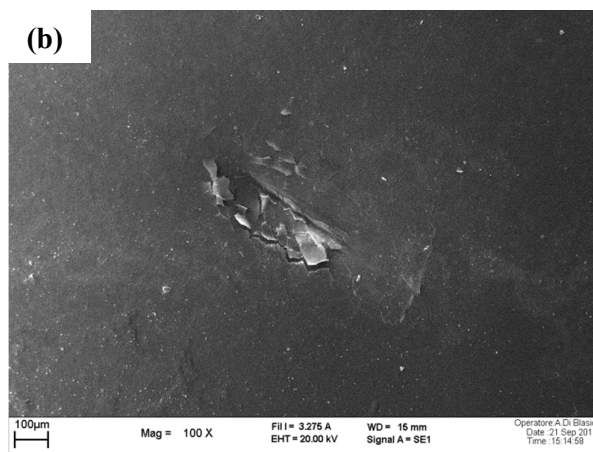
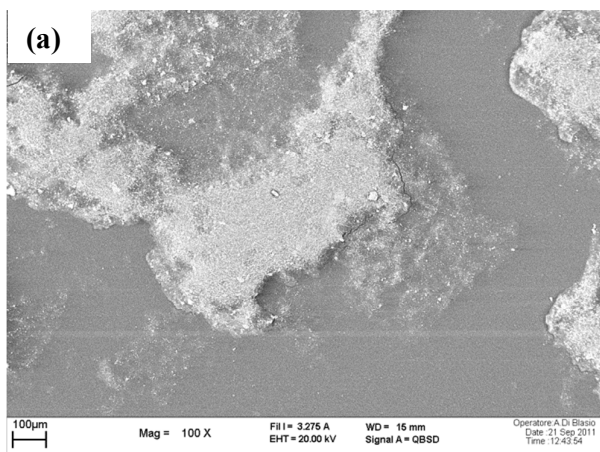


Figure 7a, b



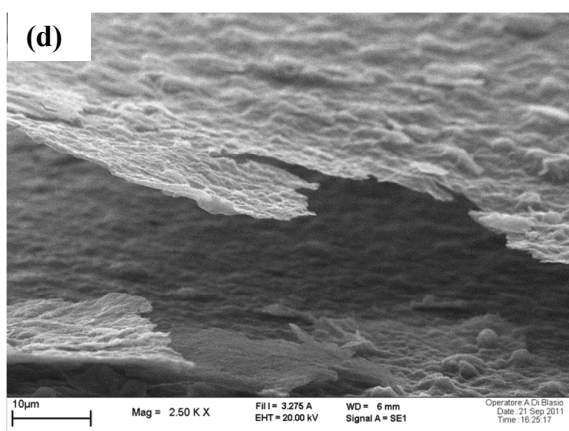
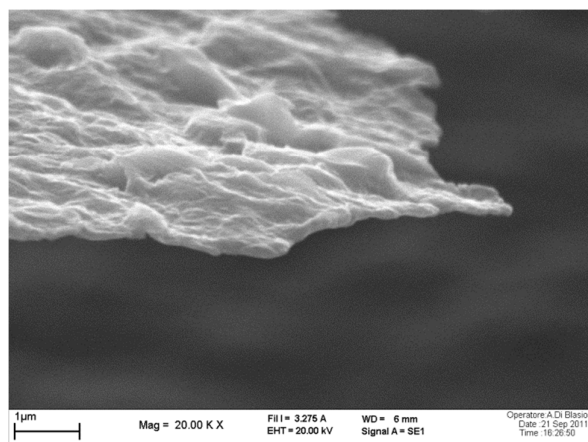
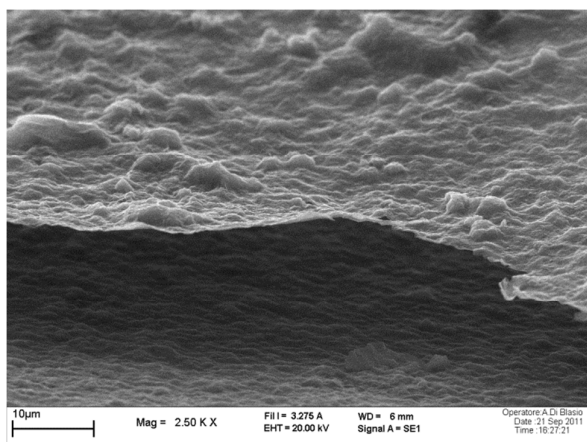


Figure 8a, b, c, d

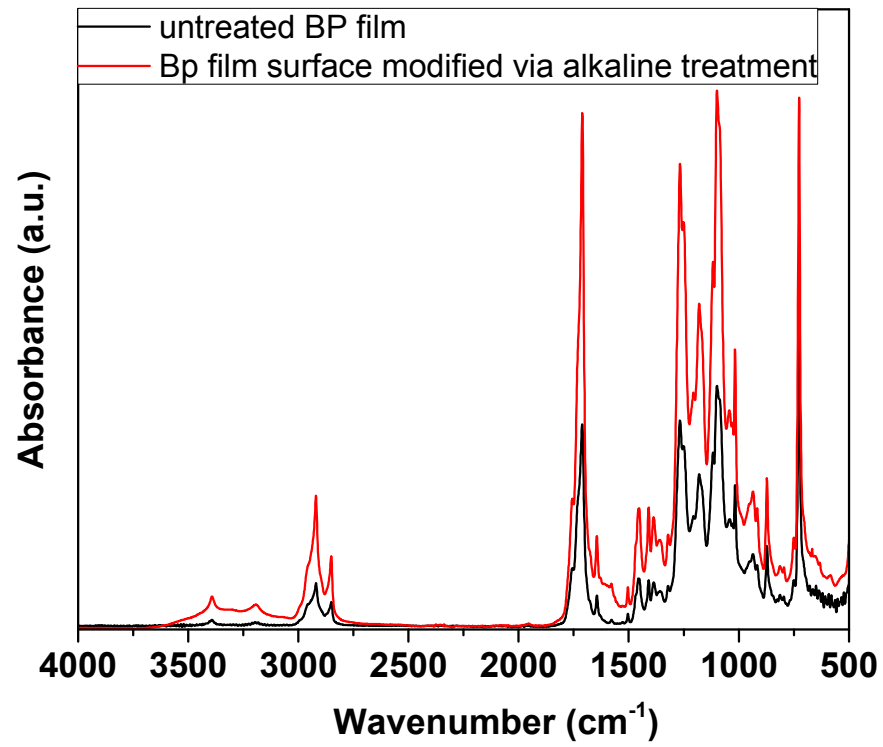


Figure 9

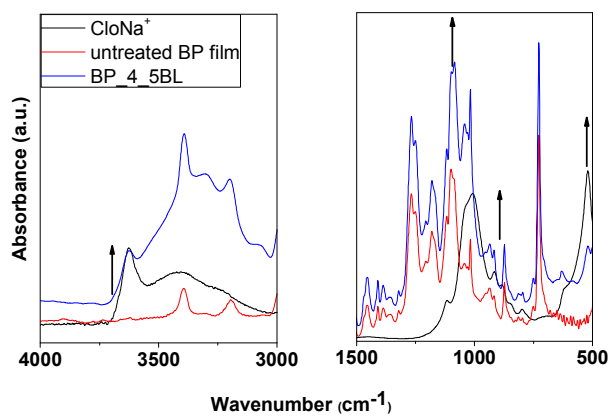


Figure 10

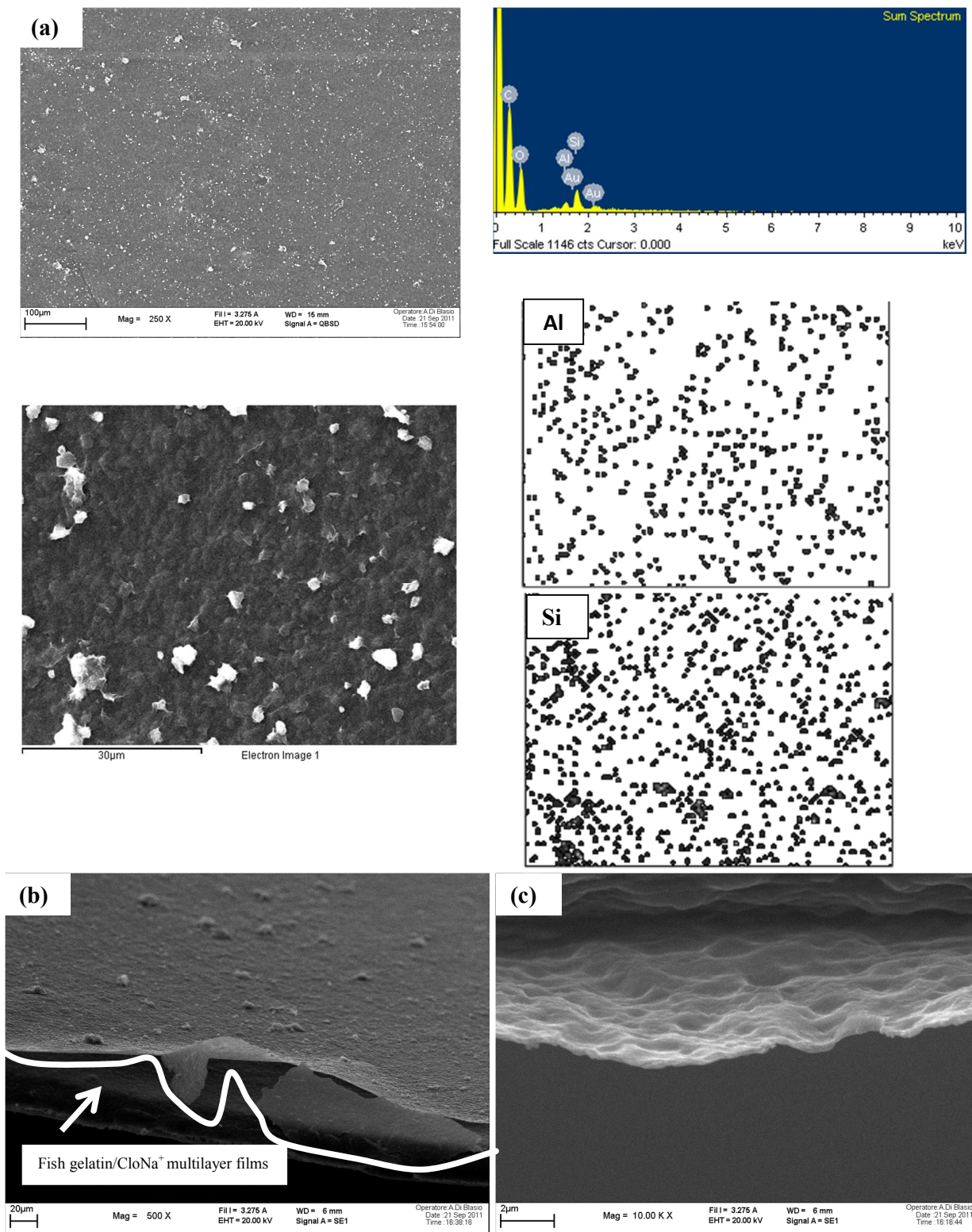
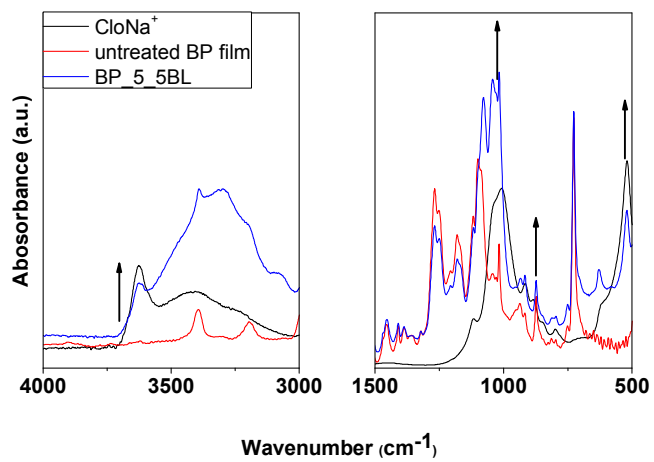


Figure 11a, b, c

**Figure 12**

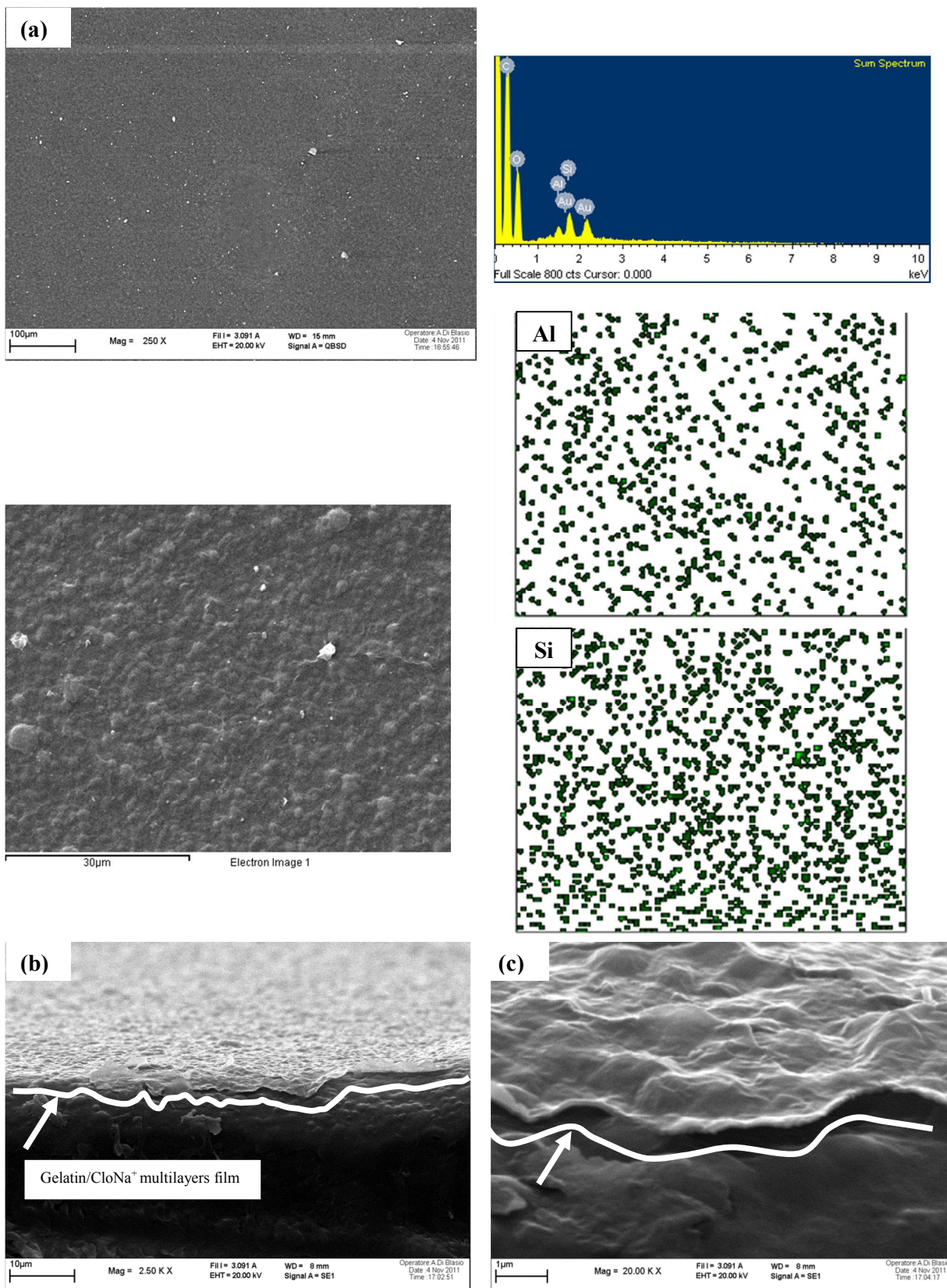
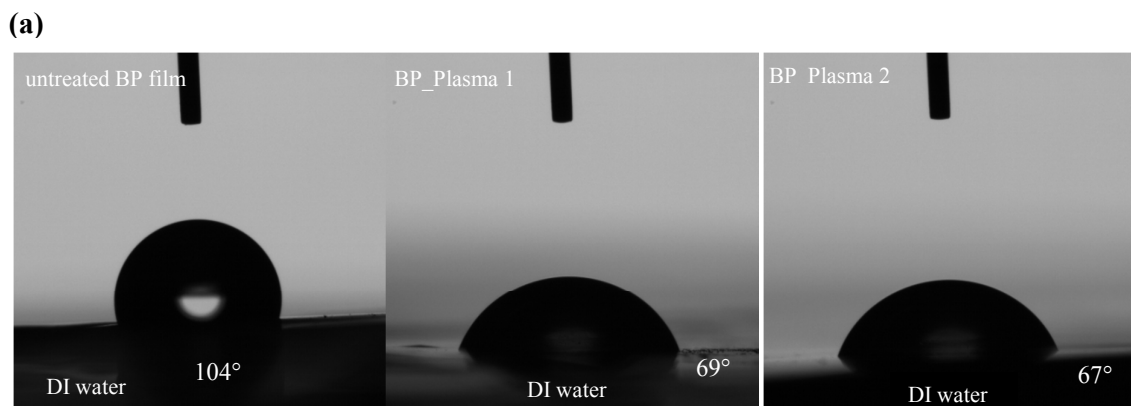


Figure 13a, b, c



(b)

Figure 14 a,b

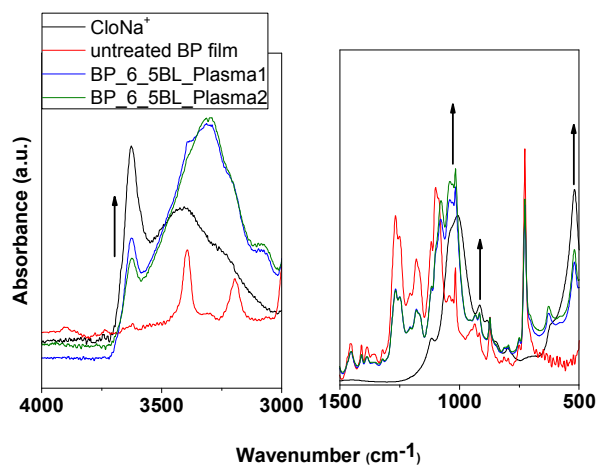
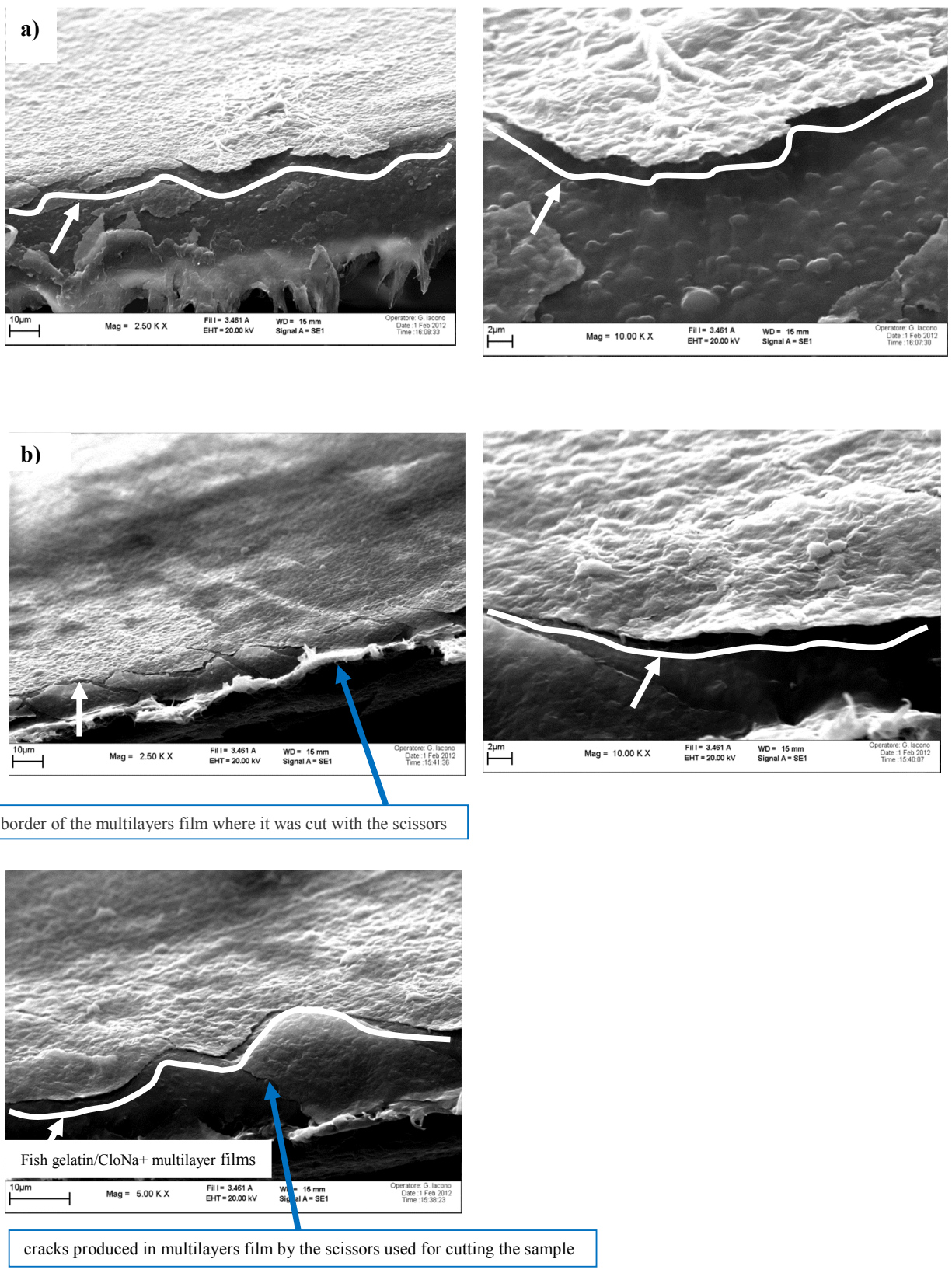


Figure 15



border of the multilayers film where it was cut with the scissors

cracks produced in multilayers film by the scissors used for cutting the sample

Figure 16 a, b

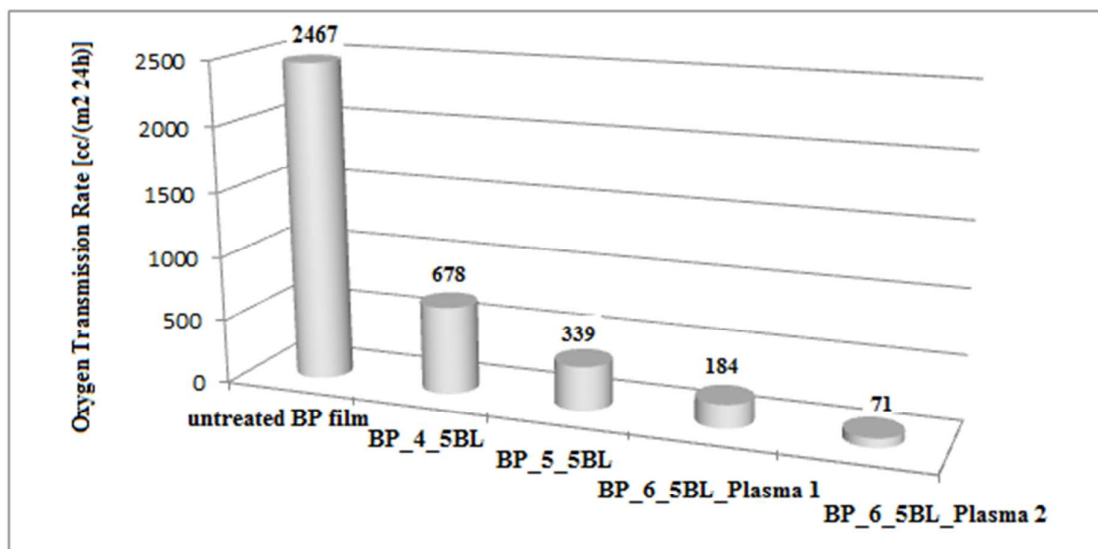


Figure 17